Development 130, 3877-3889

doi:10.1242/dev.00580

A retrospective clonal analysis of the myocardium reveals two phases of clonal growth in the developing mouse heart

Sigolène M. Meilhac, Robert G. Kelly*, Didier Rocancourt, Sophie Eloy-Trinquet, Jean-François Nicolas and Margaret E. Buckingham†

CNRS URA 2578, Département de Biologie du Développement, Institut Pasteur, 25-28 rue du Dr Roux, 75724 Paris Cedex 15, France

*Present address: Department of Genetics and Development, College of Physicians and Surgeons of Columbia University, 701 West 168th Street, New York, NY10032, USA

†Author for correspondence (e-mail: margab@pasteur.fr)

Accepted 2 May 2003

SUMMARY

Key molecules which regulate the formation of the heart have been identified; however, the mechanism of cardiac morphogenesis remains poorly understood at the cellular level. We have adopted a genetic approach, which permits retrospective clonal analysis of myocardial cells in the mouse embryo, based on the targeting of an *nlaacZ* reporter to the α-cardiac actin gene. A rare intragenic recombination event leads to a clone of β-galactosidase-positive myocardial cells. Analysis of clones at different developmental stages demonstrates that myocardial cells and their precursors follow a proliferative mode of growth, rather than a stem cell mode, with an initial dispersive phase, followed by coherent cell growth. Clusters of cells are dispersed along the venous-arterial axis of the heart tube. Coherent growth is oriented locally, with a main axis, which corresponds to the elongation of the cluster, and rows of cells, which form secondary axes. The angle between the primary and secondary axes varies, indicating independent events of growth orientation. At later stages, as the ventricular wall thickens, wedge shaped clusters traverse the wall and contain rows of cells at a progressive angle to each other. The cellular organisation of the myocardium appears to prefigure myofibre architecture. We discuss how the characteristics of myocardial cell growth, which we describe, underlie the formation of the heart tube and its subsequent regionalised expansion.

Key words: Mouse heart morphogenesis, Myocardium, Clonal cell growth, *laacZ*

INTRODUCTION

The heart, which is the first organ to form in the embryo, provides a striking example of morphogenesis (see Harvey, 2002). The cardiac precursor cells invaginate early through the rostral primitive streak during gastrulation. Subsequently, they are displaced rostrally as two bilaterally symmetrical regions of splanchnic mesoderm, which fuse below the head folds and form a crescent. This cardiac crescent, which already contains differentiated cardiomyocytes, forms an epithelial heart tube that undergoes looping, with formation and growth of the ventricular and atrial chambers and their subsequent septation. Addition of cardiomyocytes caudally continues as the cardiac tube grows. There is also a second source of cardiac precursors, located in the anterior or secondary heart field, which contributes to the arterial pole of the heart, as demonstrated for chicken (Mjaatvedt et al., 2001; Waldo et al., 2001) and mouse (Kelly et al., 2001). Although the final structure of the heart differs between vertebrates, from two chambers and a single blood flow in fish for example, to four chambers and two circulatory routes in birds and mammals (see Fishman and Olson, 1997), the initial stages of cardiogenesis are similar. Indeed regulatory genes such as *Nkx2.5* (*tinman*) or members of the *Mef2* family (*Drosophila mef2*), which are important in cardiac cell specification and differentiation respectively, are conserved even between vertebrates and invertebrates (see Cripps and Olson, 2002). Activation of the genes that determine cardiac cell fate depends upon signalling molecules from surrounding tissues: in the avian embryo, it has been shown that BMPs produced by the underlying endoderm act as inducers, while canonical Wnt signalling from the neural tube restricts the extent of the cardiogenic field (see Zaffran and Frasch, 2002). Major morphological changes take place in the vertebrate heart at the time of looping. This process is orchestrated by the left-right signalling pathway, under the influence of TGFβ family members (see Capdevila et al., 2000), which activate further regulatory genes, such as Pitx2. The divergence in the final structure of the heart between species, despite the conservation of gene networks, underlines the importance of studying cell behaviour, which is controlled by molecular signalling. Morphogenesis is the result of different types of cell behaviour, including growth, defined here as the process of cell proliferation, which is regulated temporally and ordered spatially as the embryo develops. In

mammals, such as the mouse, growth patterns are of particular interest because of the extensive cell movements which take place during embryogenesis (see Mathis and Nicolas, 2002), and because commitment to a particular cellular fate is polyclonal (see Stent, 1985). Cell labelling studies give insight into this process and provide information about the genealogical relationships between cells within a structure.

Most cell labelling experiments of myocardial precursor cells have been carried out on avian embryos. They have provided detailed fate maps for the heart (e.g. Rawles, 1943; Stalsberg and De Haan, 1969; de la Cruz et al., 1989; Redkar et al., 2001). Based on grafting and DiI labelling experiments, it has been proposed that the organisation of myocardial cells in the linear heart tube reflects their rostrocaudal origin in the primitive streak (Rosenquist and De Haan, 1966; Garcia-Martinez and Schoenwolf, 1993), and that cardiac precursor cells move from their location in the primitive streak to the more rostral position, under the head folds, as a coherent sheet (Rosenquist and De Haan, 1966; Stalsberg and De Haan, 1969). By contrast, aggregates of 10-50 cells had been observed migrating independently from one another in the cardiogenic region of chick splanchnic mesoderm (DeHaan, 1963a; DeHaan, 1963b). More recent DiI labelling experiments have indicated that there is intermingling of cells during their migration from the primitive streak, such that the organisation of cells with a pattern that reflects their position later in the heart only emerges clearly at the cardiac crescent stage (Redkar et al., 2001). At later stages, some degree of intermingling of myocytes, as monitored by retroviral labelling, has been observed across the ventricular wall after chamber formation (Mikawa et al., 1992b). In these experiments, the organisation of cells was examined and their orientation in spindle-like patterns described (Mikawa et al., 1992a).

In the mammalian heart, cell labelling and cell transplantation experiments have identified the position of cardiac precursors in the epiblast (Lawson et al., 1991) and primitive streak (Tam et al., 1997; Kinder et al., 1999), and have documented their displacement rostrally. However, little is known about cell behaviour and growth of cardiac precursors. Prior to gastrulation, cell labelling (Lawson et al., 1991) and cell transplantation (Gardner and Cockroft, 1998) experiments have shown extensive intermingling of growing cells in the mouse epiblast. As a step towards understanding the cellular basis of cardiac morphogenesis, we have examined the distribution at different developmental stages of clonally related cells in the mouse myocardium, which is the major tissue of the developing heart. We have adopted a retrospective clonal approach based on the use of an *nlaacZ* reporter gene, which is inactive unless it undergoes a rare event of spontaneous intragenic recombination, leading to the generation of a β-galactosidase-positive clone (Bonnerot and Nicolas, 1993). Because of its genetic nature, the method is non-invasive and the label, *nlacZ*, is stable. Appearance of the label is random and permits a systematic retrospective analysis, without any preconception as to the spatiotemporal localisation of the labelled precursor, which is not the case with prospective techniques such as dye labelling or grafting.

In this report, the *nlaacZ* reporter gene was targeted to an allele of the endogenous α-cardiac actin gene, which is expressed throughout the myocardium (Sassoon et al., 1988) and therefore permits a retrospective clonal analysis of myocardial cells in all regions of the mouse heart. Systematic analysis of the frequency, size and distribution of myocardial clones at different developmental stages demonstrates that these cells undergo two growth phases, which follow a proliferative rather than a stem cell mode. At earlier stages, growth is dispersive and oriented along the venous-arterial axis of the heart tube. Before embryonic day (E) 8.5, a second phase of coherent growth begins to emerge and subsequently characterises myocardial cell proliferation, both on the surface of the heart and through the thickness of the ventricular walls in an oriented way. The number and organisation of cells within clones provide new insight into how cellular growth patterns underlie the morphogenesis of the mammalian heart.

MATERIALS AND METHODS

Cloning of the targeting vector

NlaacZ1.1 is a modified bacterial *lacZ* gene designed with a nuclear localisation signal and an intragenic duplication of 1.1 kb, chosen on the basis of estimated recombination frequency and myocardial cell numbers (data not shown). *NlaacZ1.1* is derived from an *nlacZ*-pUC19 plasmid (Tajbakhsh et al., 1996a) with a *Cla*I-*Sac*I intragenic duplication corresponding to nucleotides 870-1987 after the ATG such that a shift in codon phase introduces a TGA STOP codon at nucleotide 1993, after the beginning of the duplicated sequence (Fig. 1A). *NlacZ*ΔSac is a *Sac*I-*Eco*RI fragment of *nlacZ*-pUC19, which has been ligated to a DNA fragment obtained by annealing SBE1 (5′-CCTTCGAAGCGCGCGTTCGAAGATATCCTTCGAAAGATCTG-TCGACCTCGAGG) to SBE2 (5′-AATTCCTCGAGGTCGACAGA-TCTTTCGAAGGATATCTTCGAACGCGCGCTTCGAAGGAGCT) oligonucleotides to introduce appropriate restriction sites. It was then cut with *Bst*BI and *Bgl*II and ligated to a *Cla*I-*Bam*HI fragment of *nlacZ*-pUC19.

The α-cardiac actin flanking sequences were isolated by long range PCR on mouse genomic DNA from HM1 ES cells [129/OlaHsd-derived] (Selfridge et al., 1992), extending 6 kb 5′ and 4.3 kb 3′ of exon 2. The Expand™ Long Template PCR System (Roche) was used with the paired primers AC55/AC53 for the 5′ sequence (5′-GAATTCGCGGCCGCAATGGAGGAACAGCTGAGATAAGTGA-CTGC/5′-AAGCTTGTCGACCCATGGTCTCCTCGTCGTCACAC-ATCCTGGCAC) and AC35/AC33 for the 3′ sequence (5′-AAGCTTCTCGAGGCATGCAAAGCTGTGCCAGGATGTGTGA-CGACGAG/5′-CTGCAGTTAATTAAGGTACCAGAGGGGGCTC-AGAGGATTCCAAGAAGCAC) and cloned into pGEM-T easy vector (Promega). The first seven codons of α-cardiac actin are repeated at the end of the 5′ and the beginning of the 3′ flanking sequences. The *nlaacZ1.1* reporter sequence was introduced after the first seven codons of α-cardiac actin to create a fusion protein: a *Nco*I-*Sal*I fragment of *nlaacZ1.1* was ligated to a 5′ α-cardiac actin (AC55-AC53) fragment obtained by *Not*I and partial *Nco*I digestion and introduced into an *Nco*I-*Sal*I pSKT modified vector (gift from S. Tajbakhsh), to generate the construct 5′*nlaacZ1.1*.

A positive neomycin selection cassette, flanked by two parallel loxP sites, was inserted after *nlaacZ1.1* in the same transcriptional orientation. A *Sal*I-*Not*I fragment of loxP-PGK-*Neo*^{R}-pA-loxP (gift from S. Tajbakhsh) (see Thomas et al., 1986) was ligated to a 3′ α-cardiac actin (AC35-AC33) fragment obtained by *Not*I-*Pac*I digestion and introduced into a *Pac*I-*Sal*I pSKT modified vector, to generate the construct Neo3′. *Sal*I-*Kpn*I Neo3′ was ligated to *Sal*I-*Kpn*I 5′*nlaacZ1.1*. A negative selection cassette encoding the A subunit of diphtheria toxin was introduced at the end of the 3′ flanking sequence. PGK-*DTA*-pA (gift from F. Relaix) (see Soriano, 1997) was inserted into a *Kpn*I site after the 3′ flanking sequence in a 5′-3′ transcription orientation. This resulted in a 700 bp deletion at

the 3′ end of the AC35-AC33 fragment, permitting its use as an external 3′ probe.

The final replacement targeting vector was verified by sequencing the junctions and tested for recombination by transient transfection into C2 cells (data not shown): occasional β-galactosidase-positive nuclei were observed as a result of intragenic recombination, showing that the recombined fusion protein has functional β-galactosidase activity (see Biben et al., 1996) and that the truncated β-galactosidase molecule produced from the *nlaacZ1.1* allele is inactive.

Generation of α_c-*actin*$^{+/nlaacZ1.1}$ targeted mice

The targeting vector was linearised by digestion with *Sac*II and electroporated into HM1 ES cells (Selfridge et al., 1992) as described previously (Tajbakhsh et al., 1996b), but with 15% foetal calf serum in the culture medium. Targeted cells were selected as neomycin positive by G418 resistance and as DTA negative by their survival. 115 G418-resistant ES clones were screened by Southern blotting using ^{32}P-probes (Fig. 1A), internal (300 bp of *Cla*I-*Eco*RV digested *nlacZ*, hybridising to the duplication of *nlaacZ*) and external (5′ – a 450 bp fragment at –5.4 kb from the transcription initiation site of α-cardiac actin, digested with *Hin*dIII-*Xba*I, a gift from M. Lemonnier; 3′ – a 700 bp α-cardiac actin fragment from AC33-AC35 digested with *Kpn*I) to the targeting vector. Two ES clones with a correctly targeted α-cardiac actin allele were identified (Fig. 1B-D) and injected into blastocysts [C57BL/6]. Germline transmission was obtained for one of the clones (α_c-*actin*$^{+/nlaacZ1.1Neo}$ line). In order to avoid undesirable genomic interactions at the locus (Olson et al., 1996), heterozygous α_c-*actin*$^{+/nlaacZ1.1Neo}$ males were crossed with homozygous PGK-*Cre* transgenic females (Lallemand et al., 1998) to remove the selectable marker gene (α_c-*actin*$^{+/nlaacZ1.1\Delta}$ line). α_c-*actin*$^{+/nlaacZ1.1\Delta}$ mice are indistinguishable from the α_c-*actin*$^{+/nlaacZ1.1Neo}$ mice, and both were used in the analysis and together referred to as α_c-*actin*$^{+/nlaacZ1.1}$.

The targeted mice were genotyped by PCR on DNA preparations from the tail, with a sense primer (Ol384) from the α-cardiac actin proximal promoter (5′-GCTGCTCCAACTGACCCCGTCCATCAGAGAG) and an antisense primer (Ol387) from *nlacZ* (5′-CGCATCGTAACCGTGCATCTGCCAGTTTGAG) at an annealing temperature of 57°C, or with a sense primer (GEN) from the neomycin resistance sequence (5′-ATCGCCTTCTATCGCCTTCTTGACGAGTTC) and an antisense primer (ACEX2-2) from α-cardiac actin exon 2 (5′-ACAGCTCTGGGGGCGTCATC) at an annealing temperature of 60°C.

In situ hybridisation

A 1.1 kb *nlacZ* antisense probe corresponding to nucleotides 870-1985 of the *lacZ* sequence was transcribed with T7 polymerase from a 5′*nlacZ*ΔSac pSKT modified plasmid, linearised with *Cla*I. The 5′*nlacZ*ΔSac construct was generated by the ligation of *Cla*I-*Sal*I 5′*nlaacZ1.1* and *Cla*I-*Sal*I *nlacZ*ΔSac. A 130 bp α-cardiac actin-specific probe was transcribed with T3 polymerase from the 5′ non-coding sequence of the mRNA (Sassoon et al., 1988). Whole mount in situ hybridisation was performed as previously described (Zammit et al., 2000).

Production and description of clones

The *nlaacZ* sequence produces a truncated β-galactosidase protein, which is deprived of enzymatic activity (see cloning of targeting vector above). It will only give rise to a β-galactosidase-positive cell if it undergoes an internal recombination event, which removes the duplication and eliminates the STOP codon in the sequence. This is a spontaneous event, which occurs during mitosis at a low frequency (Bonnerot and Nicolas, 1993). Descendants of a cell in which this has occurred will be detected provided that they express the α-cardiac actin gene. Thus, clones of cells can be observed directly in the heart of embryos from the *actin*$^{+/nlaacZ1.1}$ line.

As homozygous α_c-*actin*$^{-/-}$ mice are not viable (Kumar et al., 1997), heterozygous α_c-*actin*$^{+/nlaacZ1.1}$ males were crossed with superovulated wild-type females ([C57BL/6J×SJL]F1). The litters contained 50% of α_c-*actin*$^{+/nlaacZ1.1}$ embryos, as controlled by PCR of head genomic DNA from 100 E10.5 embryos (data not shown), showing the Mendelian inheritance of *nlaacZ1.1*. Embryos were staged taking E0.5 as the day after crossing (E, embryonic day of development; P, postnatal day of development). They were dissected in PBS, fixed in 4% paraformaldehyde, rinsed twice in PBS, stained in X-gal solution to reveal β-galactosidase activity (Tajbakhsh et al., 1996a) at 37°C for 12-48 hours, rinsed twice in PBS and postfixed in 4% paraformaldehyde. For better penetration of the solutions, the ventral pericardial wall was removed at E8.5 and E10.5. Hearts were isolated from the embryo after Xgal staining at E10.5 and E14.5. Before addition of X-gal, the thorax was ventrally incised at E14.5. At P7, the heart was isolated and transversally sectioned prior to X-gal staining.

Clones were observed under an Olympus binocular microscope, and photographed with a 3-CCD camera on a LEICA binocular microscope coupled to LIDA software.

Statistical analysis

The intragenic recombination of *nlaacZ* into *nlacZ* is a spontaneous, heritably transmitted and random event. The frequency of its occurrence can therefore be analysed by the fluctuation test of Luria and Delbrück (Luria and Delbrück, 1943). The number of independent recombinations that have occurred during the expansion of the pool of myocardial cells follows a Poisson distribution with the parameter μNt (μ is the rate of recombination and Nt is the total number of myocardial cells at the time of dissection). μ can be estimated to equal $-\ln(p_0)/Nt$ with p_0 the fraction of embryos with no recombined myocardial cells. The parameter of the Poisson distribution can thus be estimated to be $-\ln(p_0)$. The expected number of embryos having undergone N independent recombination events per heart (Table 2) is $N_0(\ln(Ne/N_0))^n/(N!)$, with N_0 the observed number of embryos with no recombined myocardial cells (N=0) and Ne the total number of dissected embryos at the stage under consideration (Table 1).

Mean comparisons were performed by the classical test of the normal distribution, calculating the parameter $u=(x_1-x_2)/\sqrt{(s_1^2/n_1+s_2^2/n_2)}$, where x is the mean, s the standard deviation and n the size of the sample.

Estimation of heart cell numbers by DNA quantitation

Hearts of E8.5 and E10.5 embryos were dissected and pools of 1 to 10 hearts analysed at a given stage. The pericardium was removed. Other cell types such as endocardial cells represent a minor contribution to the early embryonic heart, such that the preparation is largely derived from myocardium. DNA was extracted and purified from RNA using the DNeasy^{TM} kit (Qiagen). The quantity of DNA was measured at 260 nm using a Quartz microcuve (150 μl) with a Perkin Elmer Lambda Bio 20 spectrometer. Given the amount of DNA per diploid nucleus (~6 pg), the number of cells (nuclei) per heart was estimated using the following equation: cell number per heart=$OD\times5\times10^{-2}\times$ dilution×volume (μl)/number of hearts/6×10^{-6}. As a control, the total number of cells from a whole E10.5 embryo using this method was estimated to be in the range of 3×10^6 cells, which is similar to reported values using another method (Burns and Hassan, 2001).

Estimation of growth rate

For cells dividing exponentially, their growth rate (ρ) can be calculated such that $N=N_o2^n$ with N the number of cells at time point T, N_o the number of cells at time point t_0 and *n* the number of divisions where $n=t/\rho$ ($t=T-t_0$ is the duration of growth, i.e. 48 hours between E10.5 and E8.5).

RESULTS

Introduction of an *nlaacZ* reporter sequence into the α-cardiac actin gene

Clonal analysis of myocardial cells in the embryonic heart

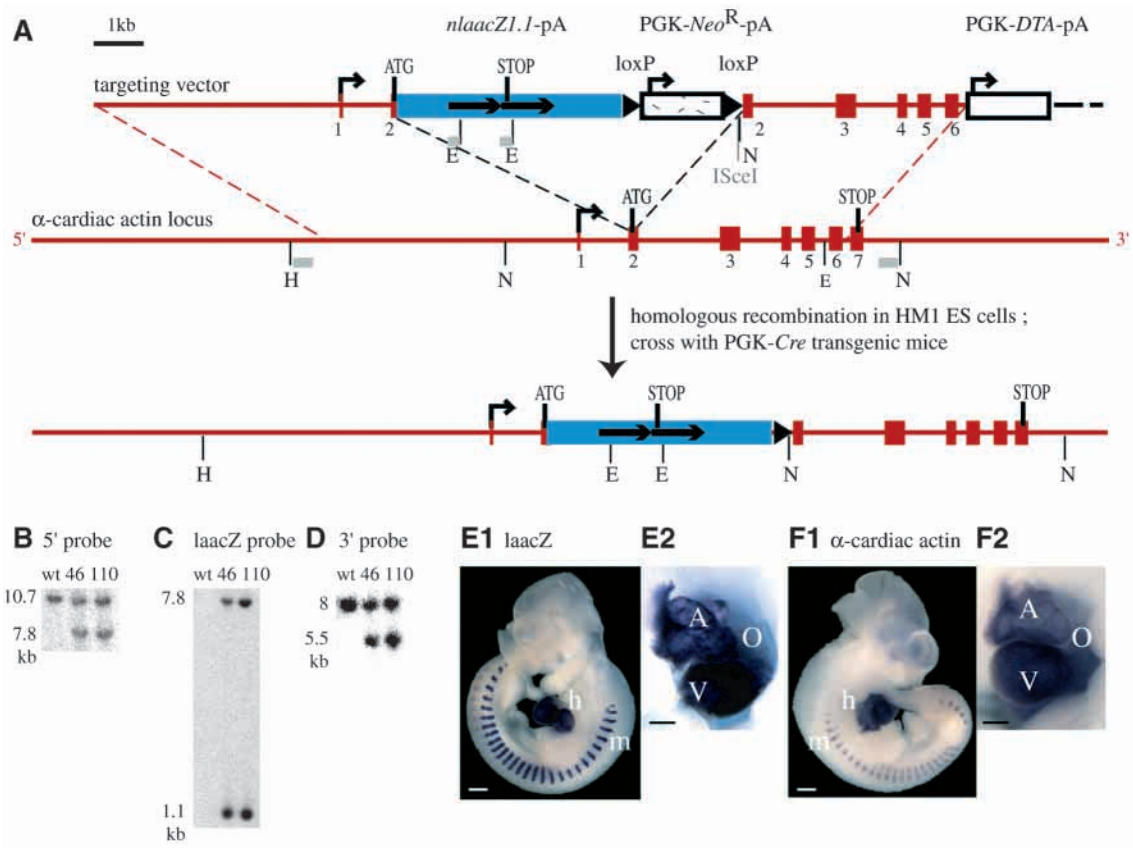

Fig. 1. Targeted integration of the *nlaacZ1.1* reporter gene into the second exon of the mouse α-cardiac actin gene. (A) Structure of the targeting vector and the α-cardiac actin locus before homologous recombination and after integration and crossing with a PGK-*Cre* transgenic mouse. Arrows at right angles show the transcriptional start sites of the α-cardiac actin promoter and PGK promoters in the selection cassettes. Numbered red boxes represent α-cardiac actin exons. Arrows in the *nlaacZ1.1* gene (blue box) indicate the position and length of the intragenic duplication (1.1 kb), which introduces a TGA STOP codon at amino acid 665. Black triangles represent loxP target sites for Cre recombinase. The PGK-*Neo*^{R} (neomycin) cassette for positive selection (speckled box) and the PGK-*DTA* (diphtheria toxin A-chain) cassette for negative selection (open box) are indicated. The *nlaacZ* and selection cassettes contain a polyadenylation sequence (pA) at their 3′ end. A site for the meganuclease ISceI was introduced immediately after the second loxP site to facilitate future manipulation of the modified locus. Probes derived from the *nlaacZ1.1* sequence and 5′ or 3′ external genomic sequences are shown below as grey boxes. E, *Eco*RV; H, *Hin*d III; N, *Nco*I. (B-D) Southern blot analysis of genomic DNA from parental ES cells (wild type) or correctly targeted clones (46, 110). The 5′ probe detects 10.7 kb and 7.8 kb bands from the wild-type and targeted alleles, respectively, after digestion with *Hin*dIII/*Eco*RV (B); the probe derived from the *laacZ* sequence detects 7.8 kb and 1.1 kb bands from the targeted allele and the *nlaacZ1.1* intragenic duplication, respectively, after digestion with *Hin*dIII/*Eco*RV (C) and the 3′ probe detects 8 kb and 5.5 kb bands from the wild-type and targeted alleles, respectively, after digestion with *Nco*I (D). (E1) Whole-mount in situ hybridisation with a probe that detects *laacZ* transcripts on an E10.5 α_c-*actin*$^{+/nlaacZ1.1}$ embryo showing expression of the targeted allele throughout the myocardium (h) and in the skeletal muscle of the myotomes (m) at this stage. (E2) magnification of right lateral view of the heart shown in E1. (F1) Whole-mount in situ hybridisation with an α-cardiac actin probe on an E10.5 wild-type embryo showing expression of the endogenous gene in the same domains. (F2) Magnification of right lateral view of the heart shown in F1. Signal intensity is lower in the wild-type compared with the targeted embryo, probably owing to the smaller size of the α-cardiac actin specific probe. Signal intensity in the heart appears lower in the outflow tract (O) and atria (A) compared with the ventricles (V) because of differential thickness of the tissue. Scale bars: 500 μm in the detailed heart views; 1 mm in the whole embryo images.

requires that an appropriate *nlaacZ* reporter sequence be placed under the transcriptional control of a gene expressed throughout the myocardium. The α-cardiac actin gene fulfils this requirement (Sassoon et al., 1988). In order to avoid position effects due to the site of transgene integration and other anomalies in expression due to the nature of transgene regulatory sequences, we chose to integrate the *nlaacZ* reporter sequence into the endogenous α-cardiac actin gene by homologous recombination (see Materials and Methods and Fig. 1A-D). Heterozygous progeny are viable, fertile and indistinguishable from wild type, with normal hearts, as previously shown for heterozygote α-cardiac actin$^{+/-}$ mice (Kumar et al., 1997). We conclude that the modified allele does not affect the development or functioning of the heart.

The *nlaacZ1.1* expression profile was verified by whole-mount in situ hybridisation with an antisense probe to detect *nlaacZ* transcripts on α_c-*actin*$^{+/nlaacZ1.1}$ embryos at embryonic day (E) 10.5 (Fig. 1E1-E2), and compared with hybridisation with an antisense α-cardiac actin probe on wild-type E10.5 embryos (Fig. 1F1-F2). As expected from the transcription profile of the α-cardiac actin gene (Sassoon et al., 1988), *nlaacZ1.1* is expressed throughout the myocardium and in the skeletal muscle of the myotomes at this stage. Observation of X-gal-positive clones throughout the myocardium at E8.5, as

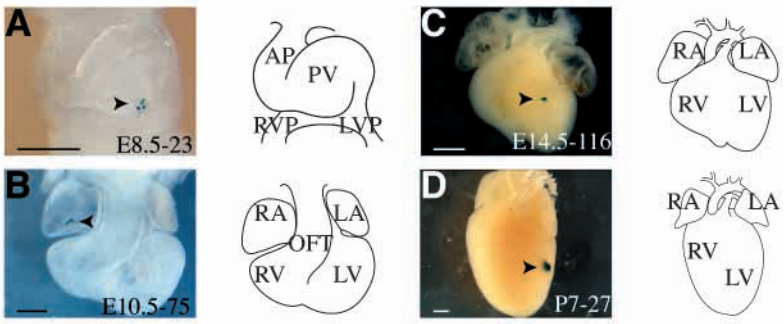

Fig. 2. Examples of hearts with a small number of β-galactosidase-positive cells. Ventral views of E8.5 (A), E10.5 (B), E14.5 (C) and P7 (D) α_c-*actin*$^{+/nlaacZ1.1}$ hearts coloured by X-gal to reveal the distribution of cells containing a recombined *nlacZ* allele (first column of panels). Each blue dot represents a single nucleus since the reporter gene contains a nuclear localisation signal. At higher magnification and by changing the focus, it is possible to obtain reliable counts of β-galactosidase-positive cells at E8.5 and E10.5. Arrowheads show that labelled cells form coherent clusters. Schematic representations of hearts at these stages indicate the cardiac subregions (second column of panels). The numbers in the lower right corner of the panels indicate the stage followed by the identification number of the positive embryos. AP, arterial pole; LA, left atrium; LV, left ventricle; LVP, left venous pole; PV, primitive ventricle; RA, right atrium; RV, right ventricle; RVP, right venous pole; OFT, outflow tract. Scale bars: 500 μm.

well as in the skeletal muscles at E14.5 and seven days after birth (P7), confirmed the correct expression of the reporter gene at other stages. The α_c-*actin*$^{+/nlaacZ1.1}$ mice that we have generated are thus suitable for clonal analysis of developing cardiac muscle cells.

Production of embryos with clones in the myocardium

For systematic analysis of cardiac precursor cells, a large number of random clones is required. Clones were compared at different developmental stages, as illustrated in Fig. 2: at E8.5, an early stage of cardiogenesis when the heart is a looped tube (Fig. 2A), at E10.5, when the heart is still a non-septated tube, but when the different cardiac chambers can be identified morphologically (Fig. 2B), at E14.5, when ventricular septation is complete and trabecular remodelling is under way (Fig. 2C) and at P7, when morphogenesis of the heart is complete (Fig. 2D). One thousand four hundred and thirty three embryos or neonates, dissected at these developmental stages, had β-galactosidase-positive cells in the heart and are described here (Table 1).

As expected, the frequency of embryos with β-galactosidase-positive cells increases with age (Table 1), reflecting expansion of the pool of α-cardiac actin-expressing cells and their precursors, and hence the number of cell divisions during which the *nlaacZ1.1* allele can undergo intragenic recombination.

At E14.5 and P7, because of the thickness of the tissue, it was not possible to obtain an accurate count of the number of labelled cells, but their organisation was documented. At E8.5 and E10.5, positive hearts were analysed for the number of β-galactosidase-positive cells and their distribution in clusters.

Clonal relationship between β-galactosidase-positive cells

As cell labelling is a random event of intragenic recombination of *nlaacZ* into *nlacZ*, the clonality between β-galactosidase-positive cells can be statistically assessed. We have calculated the expected number of embryos containing independent recombination events in the heart, at E8.5 and E10.5 (Table 2), based on the fluctuation test of Luria and Delbrück (Luria and Delbrück, 1943). A common feature of positive hearts at every stage studied is the organisation of β-galactosidase-positive cells into clusters (Figs 2, 3). To assess whether these clusters resulted from independent events of recombination, we have compared the observed distribution of the number of clusters per heart with the calculated distribution of the number of independent events of recombination per heart.

Table 1. Total number of embryos or neonates observed

Stage	Number of α_c-*actin*$^{+/nlaacZ1.1}$ embryos or neonates	Number of β-gal-positive hearts (%*)
E8.5	1488	112† (7.5%)
E10.5	641	430 (67%)
E14.5	627	595 (95%)
P7	316	316 (100%)

*% is the number of β-gal-positive hearts divided by the number of α_c-*actin*$^{+/nlaacZ1.1}$ embryos or neonates.
†Ninety-two hearts from embryos with 9-17 somites are analysed here.

At E8.5, few observations of polyclonality are expected (more than one independent recombination event, Table 2). They probably correspond to the few cases (n=6) in which one or two cells are isolated from the other β-galactosidase-positive cells (white arrow in Fig. 3D1). Note also that in hearts with multiple clusters, the average number of cells per cluster is significantly higher than that in hearts with a single cluster (5.2±s.e.m. 0.5, n=69 versus 3.2±s.e.m. 0.5, n=59: u=2.76, P<0.01), whereas we would expect these numbers to be similar if multiple clusters resulted from independent recombination events.

At E10.5, the observed and expected distributions differ significantly as N increases (Table 2), demonstrating that clusters of β-galactosidase-positive cells may be clonally related. Two independent labelling events will more probably be located in different regions and have a disparate organisation. In addition, they will more probably lead to smaller clusters as 90% of the positive hearts at E10.5 contain less than 17 labelled cells. Therefore, large clusters, which are closely associated (two clusters of 18 and 32 cells in the outflow tract Fig. 3E) or aligned (seven clusters of more than 20 cells Fig. 3G; this alignment was found in two hearts) are considered to be clonally related.

Similarly, at E14.5 and P7, small clusters are more frequent. Therefore, large clusters closely associated (Fig. 3F) or reproducibly aligned are considered to be clonally related.

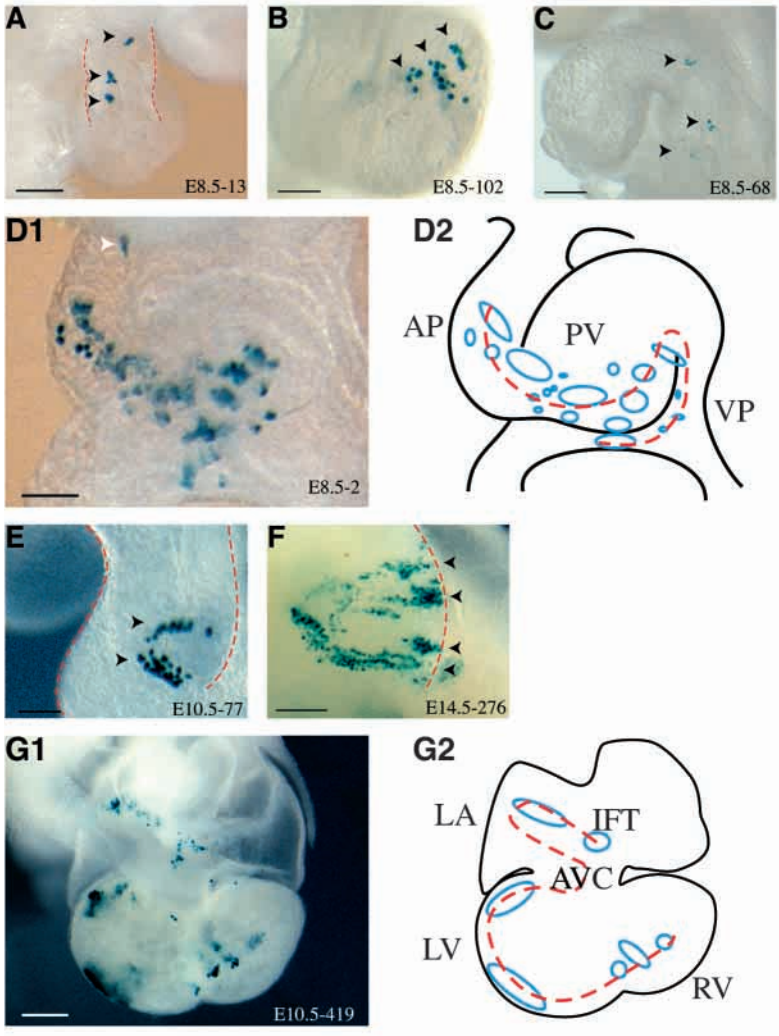

Fig. 3. Examples of hearts with multiple clusters. β-galactosidase-positive hearts at E8.5 with at least three β-galactosidase-positive clusters (black arrowheads), which are clonally related (see text), are shown in the arterial pole (AP) of the cardiac tube (A), in the primitive ventricle (PV) (B), in the venous pole (VP) (C) or throughout the cardiac tube (D). The white arrowhead in D1 shows two isolated cells that may not be clonally related to the others. D2 is a schematic representation of the clusters (blue open circles show location along the axis of the tube) in the heart at E8.5 with an exceptionally large number of labelled cells (82) presented in D1. Later, large and closely associated clusters, which are clonally related (see text), are shown in the outflow region at E10.5 (E), and E14.5 (F). A heart at E10.5, with an exceptionally large number of labelled cells (420), contains seven clusters of more than 20 cells (G1) and is schematised in G2. Dispersion of the clusters is parallel to the venous-arterial axis of the cardiac tube (broken red lines). Note the increase in the relative sizes of the clusters with age. In all panels, the orientation is cranial (upwards) to caudal (downwards). (A) Right lateral view; (B,D-F) Ventral views; (C) Left lateral view; (G) Dorsal view. AVC, atrioventricular canal; IFT, inflow tract; LA, left atrium; LV, left ventricle; RV, right ventricle. Scale bars: 200 μm.

Myocardial cells undergo two growth phases

The distribution of β-galactosidase-positive cells is not homogenous and cells tend to be organised into clusters. This is a common feature of positive hearts at every stage studied and in all cardiac subregions. They are classified into two categories: hearts with a single cluster (Fig. 2) or with multiple (>1) clusters (Fig. 3). The organisation into clonally related clusters shows that myocardial cells undergo two growth phases, one that is characterised by cell dispersion, leading to the separation of the clusters, and another that is coherent, i.e. cells remain close to one another after division, leading to the formation of a cluster.

Timing of the growth phases

To understand the timing of the growth phases, the simplest model is to consider that dispersion precedes coherence. In this way, hearts with multiple clusters reflect a recombination event in an early precursor and hearts with a single cluster in a recent precursor. Alternatively, if coherence precedes dispersion, the existence of hearts with a single cluster can only be explained if the precursors of these clones have not undergone the second (dispersive) phase, because they have different growth properties (quiescence or a single growth phase). Furthermore, if dispersion is late, we would expect that in hearts with multiple clusters, clusters would have a smaller size at E10.5 than at E8.5. In fact, this is not the case. Hearts with a large number of cells colonising several cardiac subregions were detected (two hearts at E8.5 and five at E10.5). In these hearts, the size of the clusters as well as the distance between the clusters increases significantly between E8.5 and E10.5 (Fig. 3D at E8.5 and Fig. 3G at E10.5). Furthermore, the distinction between clusters at E8.5 is not always clearly evident (in eight hearts), whereas it is evident at E10.5, indicating that even in these E8.5 hearts, clusters are in fact distinct, although this only becomes obvious later. Other examples in the

Table 2. Statistical analysis of clonality at E8.5 and E10.5

	Number of E8.5 hearts*		Number of E10.5 hearts	
N	Observed with N β-gal-positive clusters	Expected with N independent recombination events	Observed with N β-gal-positive clusters	Expected with N independent recombination events
0	1376		211	
1	59	108	215	234
2	15	4	120	130
3	5	0.1	60	48
4	2	2×10^{-3}	22	13
5	2	3×10^{-5}	7	3
6	1	4×10^{-7}	3	1
7			2	0.1
⩽				
12			1	2×10^{-6}

We have tested whether multiple clusters within a heart resulted from independent recombination events. The observed distribution of the number of clusters per heart is compared with the expected random distribution, based on the fluctuation test of Luria and Delbrück (see Materials and Methods).

*Eight positive hearts at E8.5, in which clusters were not clearly distinguishable, were excluded from the observed distribution.

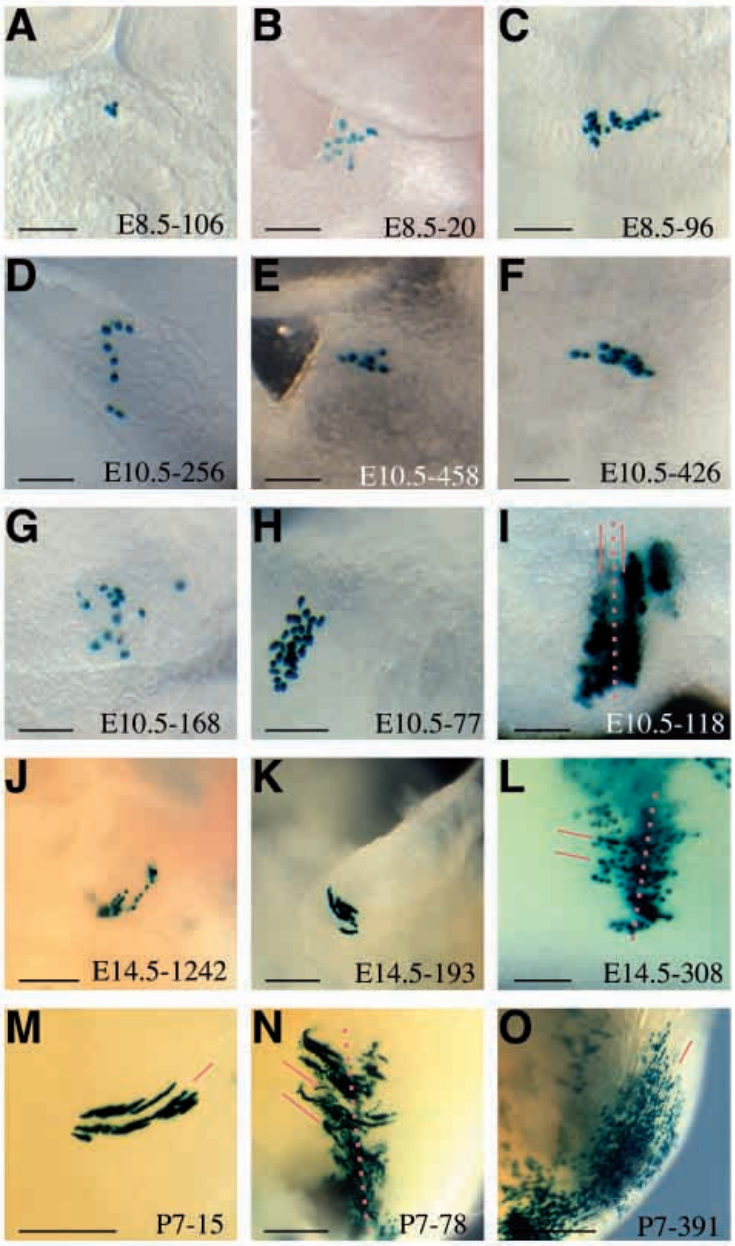

Fig. 4. Organisation of coherent clusters observed on the surface of the heart. Examples of clusters viewed at the surface of the heart are shown at stages E8.5 (first line of panels), E10.5 (second and third lines of panels), E14.5 (fourth line of panels) and P7 (fifth line of panels). Low level of intermingling between unlabelled (*nlaacZ* genotype) and labelled (*nlacZ* genotype) cells is observed. The main axis of the clusters is represented in three examples (I,L,N) by a broken red line. The axes of rows of cells within a cluster are represented in the same examples by unbroken red lines. In M and O, the unbroken red line outlines the orientation of cardiac myofibres at P7, which lie parallel to the rows of labelled cells. At P7, the staining often appears as an elongated unit (M-N), in contrast to the dotted nuclei in other panels, probably reflecting the leakage of β-galactosidase to the cytoplasm, either during the binucleation of cardiomyocytes or because of a saturation of the staining. (A,C) The primitive ventricle; (B) the venous pole; (D,K,N) the atria; (E) the atrioventricular canal; (F,I,L,M,O) the ventricles; (G,J) the inflow tract; (H) the outflow tract. (A,B) Hearts with a single cluster. Scale bars: 200 μm.

same cardiac region at different stages (Fig. 3A at E8.5, Fig. 3E at E10.5 and Fig. 3F at E14.5) also illustrate the increase in the size of the clusters. Quantitatively, the average number of cells per cluster significantly increases from E8.5 to E10.5 in hearts with multiple clusters (5.2±s.e.m. 0.5, n=69 versus 8.3±s.e.m. 1.1, n=587: u=2.65, P<0.01), in spite of the underestimation at E10.5, which is due to independent events of recombination resulting in additional small clusters (see discussion of clonal relationship and Table 2). Together, these observations suggest that clones with multiple clusters develop coherently (increase in the size of the clusters), so that coherent growth predominates after E8.5.

Geometry of clones during the dispersive growth phase

Characterisation of the dispersive growth phase was performed by analysing clones with multiple clusters. At E8.5, dispersion between clusters is observed in the different cardiac subregions, arterial pole (n=5, Fig. 3A), primitive ventricle (n=8, Fig. 3B) and venous pole (n=8, Fig. 3C), as well as between them (n=12, Fig. 3D). The direction of dispersion can be assessed by analysing the spatial relationship between clusters. In 26/33 (80%) of E8.5 hearts with multiple clusters, these are aligned along the venous-arterial axis of the cardiac tube, which initially has a rostrocaudal orientation (broken red lines Fig. 3A). This remains true at later stages, as shown for adjacent clusters in the outflow region (Fig. 3E at E10.5 and Fig. 3F at E14.5, compared with Fig. 3A at E8.5).

The direction of dispersion can also be assessed by analysing the full extension of a clone. In embryonic hearts with a large number of β-galactosidase-positive cells (Fig. 3D at E8.5 and Fig. 3G at E10.5), the staining extends all along the venous-arterial axis of the tube whereas there is only partial extension along the perpendicular circumferential axis. This shows that myocardial cell growth is anisotropic and that clonally related myocardial cells are distributed along the venous-arterial axis of the tube.

Geometry of clones during the coherent growth phase

Characterisation of the coherent growth phase was performed by analysing individual clusters. Coherent clusters are found in every cardiac subregion: in the outflow tract (Fig. 4H), the ventricles (Fig. 4A,C,F,I,L,M,O), the venous pole or atria (Fig. 4B,D,K,N), the atrioventricular canal, which is best seen at E10.5 between ventricles and atria (Fig. 4E), and the inflow tract or sinus venosus (Fig. 4G,J).

On the surface

From E8.5 to P7, clusters expand on the surface of the cardiac tube. Within a cluster, β-galactosidase-positive cells are, most often, immediately adjacent (as examples see Fig. 4A,I) or, less frequently, separated by a few intercalated negative cells (see Fig. 4B,G), showing that there is a low level of intermingling

between clonally unrelated myocardial cells during this growth phase. At every stage, the overall shape of the cluster is elongated (Fig. 4C at E8.5, Fig. 4F at E10.5, Fig. 4L at E14.5 and Fig. 4O at P7), indicating that coherent growth is oriented. From E10.5, the clusters seem to be subdivided into rows of cells, a phenomenon which is observed in every cardiac subregion (Fig. 4H in the outflow tract, Fig. 4L in the ventricle, Fig. 4E in the atrioventricular canal, Fig. 4K in the atrium and Fig. 4J in the inflow tract). At P7, these rows of cells appear to be parallel to the myofibres (Fig. 4M,O). The angle between the main axis of elongation of the whole cluster and the axis of the rows of cells within the cluster is not the same in different clusters (0° in Fig. 4I, 45° in Fig. 4N, 90° in Fig. 4L), suggesting that two distinct events of oriented growth are occurring simultaneously during growth of a cluster.

On the transmural axis

Thickening of the myocardium, particularly in the ventricles, is observed morphologically from E10.5 to birth. Hearts with large ventricular clusters of β-galactosidase-positive cells were bisected transversally through the cluster (Fig. 5A2-E2 and 5C3-D3). As at the surface, β-galactosidase-positive cells are, most often, immediately adjacent within a transmural cluster (Fig. 5E2) or, less frequently, separated by a few intercalated negative cells (Fig. 5B2) showing that a low level of intermingling between clonally unrelated myocardial cells also takes place on the transmural axis. Clusters colonising the whole depth of the ventricle were observed from E10.5 to P7 (Fig. 5A at E10.5, Fig. 5B-D at E14.5 and Fig. 5E at P7), traversing both compact and trabeculated myocardium (Fig. 5B-D), indicating that both these layers of the myocardium are clonally related. Such clusters are wedge shaped, with a wider outer (towards the epicardium) side and a narrower inner (towards the endocardium) side (Fig. 5E2). Interestingly, the tip of the wedge was sometimes observed to extend into the muscular region of the interventricular septum, traversing the ventricular cavity, which appears as a discontinuity in the labelling (Fig. 5A2-B2). This observation suggests that the muscular region of the interventricular septum and the trabeculations are clonally related. The overall orientation of the clusters in the transmural axis is oblique relative to the plane of the surface (Fig. 5C1), showing that the direction of transmural growth is not perpendicular to the plane of the surface. Moreover, the orientation of the axes of the rows

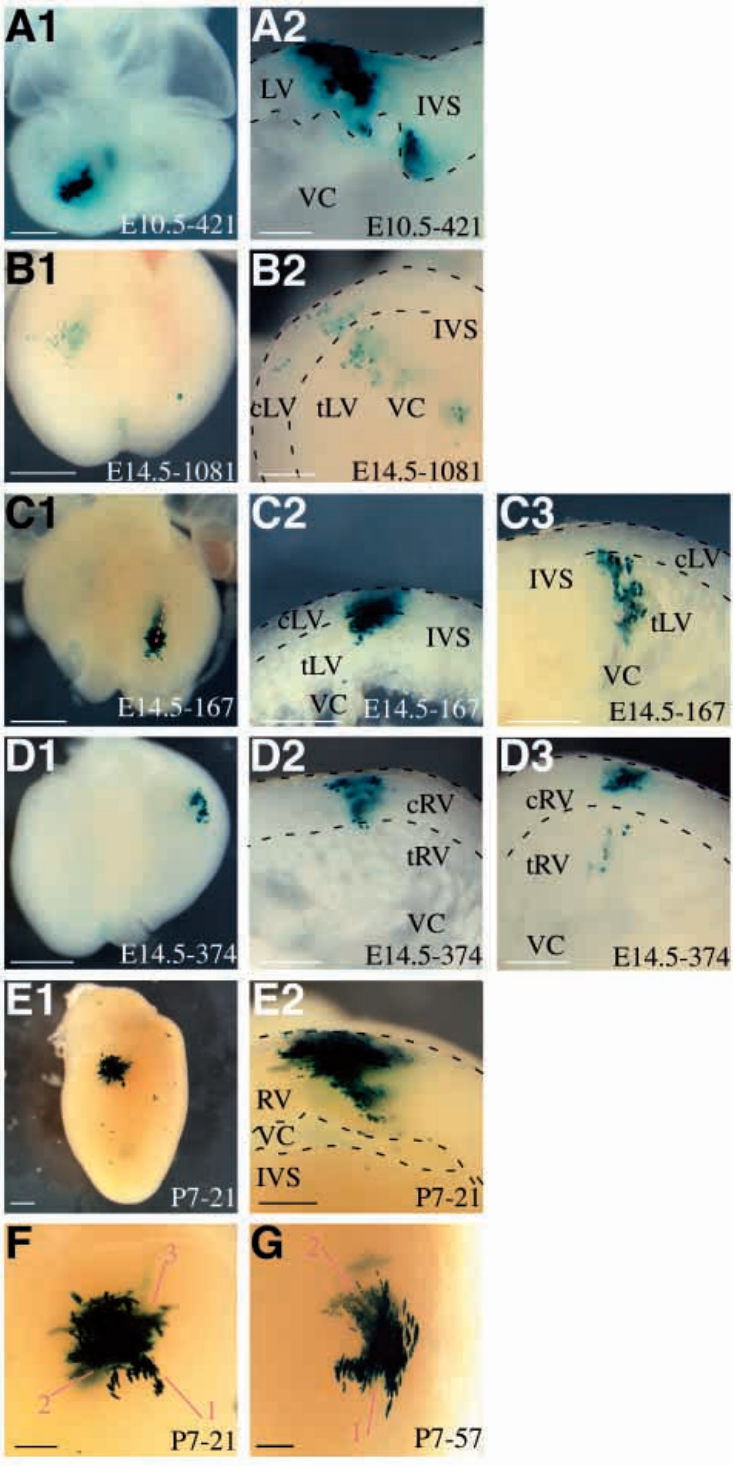

Fig. 5. Organisation of coherent clusters observed through the thickness of the ventricular wall from E10.5. Examples of large clusters viewed at the surface (A1-E1,F,G) and on the transverse plane of bisected hearts (A2-E2,C3-D3) are shown at stages E10.5 (A), E14.5 (B-D) and P7 (E-G). C2-C3 and D2-D3 each show the two sides of a transverse cut. In C1, the projection on the surface of the main transmural axis of the cluster is represented by a broken red line. In F,G, the axes of the rows of cells within a cluster are represented by red continuous lines, numbered from the outside inwards (the inner rows appear increasingly out of focus and lightly stained). (E1) Right lateral view. (C1) Ventral view. (A1,B1,D1) Dorsal views. In all sections, the epicardial (outer) side is at the top of the panel and the endocardial (inner) side is at the bottom. Broken black lines indicate the outline of epicardial and endocardial surfaces, when these were not too folded. At E14.5, these contours correspond also to the separation between compact and trabeculated ventricular myocardium. G is in the right ventricle. IVS, interventricular septum; cLV, compact left ventricle; cRV, compact right ventricle; tLV, trabeculated left ventricle; tRV, trabeculated right ventricle; VC, ventricular cavity. Scale bars: 500 μm in A1-E1; 250 μm in the other panels.

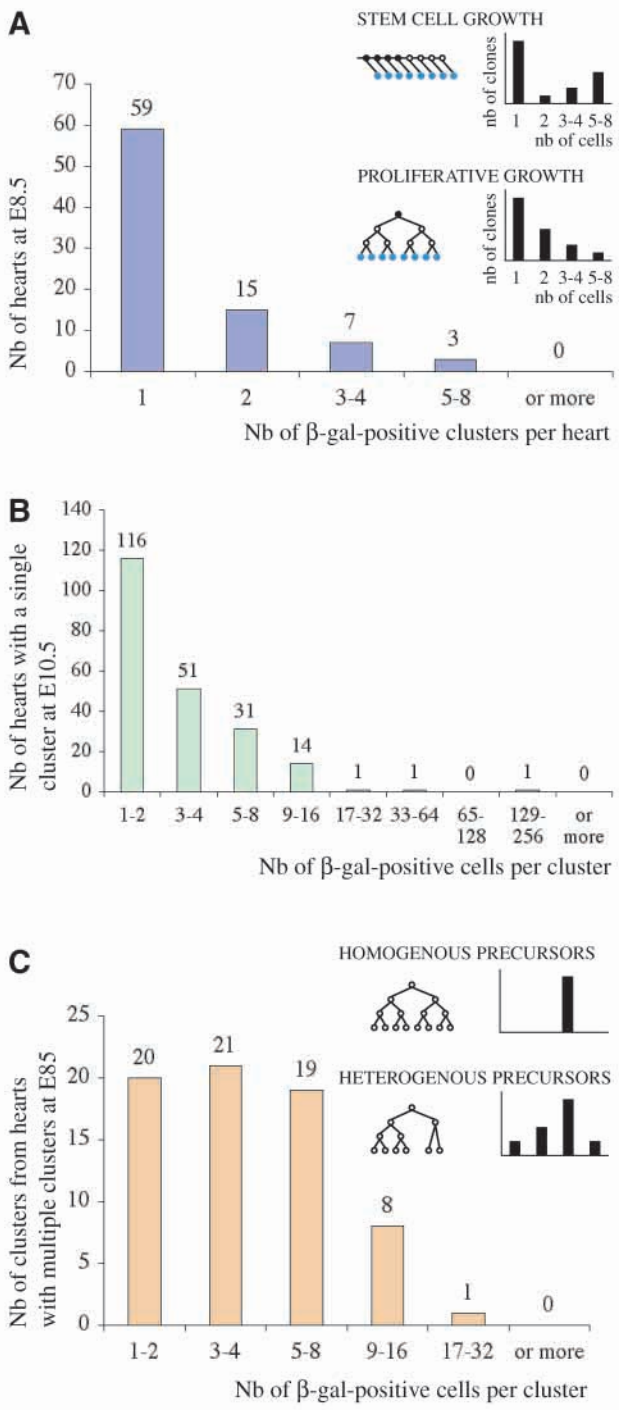

Fig. 6. Mode of growth of myocardial cells. (A) Distribution of the number of β-galactosidase-positive clusters per heart at E8.5, as an indication of the mode of growth of the dispersive phase, i.e. of the precursors of the clusters. Theoretical models of growth (adapted from Nicolas et al., 1996) are presented in the inset, including lineage relationships between cells and the predicted distribution of clone size. In a stem cell growth mode, the pool of precursor cells (in black in this example), which generate large clones (five to eight cells) is bigger than in a proliferative mode, and therefore larger clones are much more frequent. All hearts from embryos of 9-17 somites, in which clusters were clearly distinguishable, are taken into account (n=84). (B) Distribution of cluster size in hearts with a single cluster at E10.5, as an indication of the mode of growth of the coherent phase (compare with inset in A). All hearts with a single cluster at E10.5 are taken into account (n=215). (C) Distribution of cluster size in hearts with multiple clusters at E8.5, as an indication of the number of cell divisions from the initiation of the coherent growth phase to E8.5. Theoretical models of growth are presented in the inset. All hearts with multiple clusters from embryos of 9-17 somites, in which clusters were clearly distinguishable, are taken into account (69 clusters).

of cells within a cluster often appears to be staggered between more superficial rows and deeper rows (Fig. 5F-G), indicating that the orientation of the rows of cells within a cluster is not necessarily constant between layers of cells within the ventricular wall.

Mode of division during each growth phase

Two major modes of cell division can be distinguished: stem cell growth versus proliferative growth (Nicolas et al., 1996). Cardiomyocytes, unlike skeletal myocytes, are known to continue to divide after the onset of differentiation (Rumyantsev, 1977). Therefore, a proliferative mode of growth is probable at the time of myocyte differentiation; however, prior to this, stem cell growth may well intervene in the precursor cell population and contribute to heart tube elongation. Clonal analysis provides an important tool for investigating the mode of division of myocardial cells and their precursors, as it influences the distribution of clone sizes: larger clones, which result from an increasing number of cell divisions, are much more frequent in a stem cell growth mode than in a proliferative mode (inset Fig. 6A), owing to the self renewal of the recombined precursor cell, which continues to generate β-galactosidase-positive progeny.

To examine the mode of growth of myocardial precursor cells during the dispersive phase, precursors of the clusters were considered. Hearts with multiple clusters at E8.5, when few events of polyclonality are expected (Table 2), were analysed for the distribution of their number of clusters (Fig. 6A). This shows a proliferative mode during the dispersive phase. To examine the mode of growth of myocardial cells during the coherent phase, cells which have only undergone this phase were considered. Therefore hearts with single clusters at E10.5, when the size of the sample is higher, were analysed for the distribution of their number of labelled cells (Fig. 6B). This also shows a proliferative mode during the coherent phase, which is characterised by a declining frequency of large clusters (see inset Fig. 6A). The distribution does not follow a strict exponential, consistent with a probable non-constant growth rate between myocardial cells as cardiogenesis proceeds.

Given the proliferative mode of growth of myocardial cells and their precursors, as well as the timing of the phases, we predict that labelling of an earlier precursor will result in a clone with a higher number of cells and a higher number of clusters. Indeed at E8.5, hearts with a higher number of β-galactosidase-positive cells tend to have a higher number of clusters (compare Fig. 3D with 3A). Conversely, 39/56 (70%) of hearts at E8.5 with a low number of β-galactosidase-positive cells (2-16 cells) have a single cluster [Fig. 2A and Fig. 4A (clones of one cell are not considered because they can only have one cluster)].

We have also examined the contribution of the different

precursors of the clusters. Clusters born at the same time were considered, i.e. those from hearts with multiple clusters. Because labelling in these hearts dates back to the dispersive growth phase, their clusters must have been born at the time of coherent growth initiation. If precursors of the clusters had similar growth properties (i.e. underwent the growth transition synchronously and had the same coherent growth rate), we would expect the size of clusters from hearts with multiple clusters to be constant (inset Fig. 6C). This is not the case at E8.5 (Fig. 6C); therefore we conclude that myocardial precursor cells have heterogeneous growth properties, either different growth rates or different timing for the growth transition. Consistently, hearts at E8.5 with a low number of β-galactosidase-positive cells (2-16) show coherent growth (39/56 have a single cluster, see the 16 cells in Fig. 4B) or dispersive growth (17/56 have multiple clusters, see the 11 cells in Fig. 3C) and this difference is seen between hearts with the same total number of labelled cells, indicating that precursors of clones, which have undergone the same number of cell divisions, have heterogeneous growth properties.

Quantitatively, the apparent growth rate of myocardial cells was estimated between E8.5 and E10.5, when growth is proliferative. With the approximation that the rate is constant, it was calculated on the basis of the exponential increase in total myocardial cell number (see Materials and Methods). The total number of cells in the myocardium was estimated by DNA quantitation to be 19,000 cells±s.d. 4,000 at E8.5 and 180,000±s.d. 25,000 at E10.5. This gives an apparent growth rate for myocardial cells of about 15 hours±2 per cell cycle. This is only an approximation, as growth rates are lower in some areas of the looping heart such as the inner curvature, as shown in the chick embryos by Thompson et al. (Thompson et al., 1990). The 9.5-fold increase in the total number of myocardial cells is confirmed in our clonal analysis by the similar increase in the maximum size of clusters from hearts with multiple clusters (27 at E8.5 and 270 at E10.5) and in the frequency of β-galactosidase-positive embryos from E8.5 to E10.5 (Table 1). This latter observation also confirms that *nlaacZ* intragenic recombination is a random, non-biased, event.

DISCUSSION

The retrospective clonal approach described here allows analysis of the distribution of cells, descended from a precursor cell that underwent a stable genetic modification as a random event at any time or location during the development of the embryo. As the *nlaacZ* reporter is targeted to the α-cardiac actin gene, expressed throughout the myocardium, it is this major component of the heart which is monitored. The frequency of recombination, which leads to a functional *nlacZ* gene, is crucial in determining clonality. Because it is a random event, the clonality of a pattern of cell distribution can be statistically assessed. In this study, we show that most clusters of β-galactosidase-positive cells in the heart are clonally related at E8.5; this is also the case for large clusters, which are adjacent or aligned, at later stages. Our analysis demonstrates that myocardial cells and their precursors in the mouse embryo follow a proliferative mode of growth, rather than a stem cell mode, with two distinct behaviours: an earlier phase of extensive cell intermingling, when clusters of cells are dispersed along the venous-arterial axis of the cardiac tube (which initially has a rostrocaudal orientation), followed by oriented coherent cell growth, which is characterised by a low level of intermingling.

Early rostrocaudal dispersion of myocardial cell precursors

The growth properties of myocardial cell precursors during the dispersive growth phase underlie the cellular basis of heart tube formation. We have not detected characteristic stem cell growth during this early phase. The heart tube is a polyclonal structure, in which rearrangement of clones occurs along the venous-arterial axis, probably because of intercalation.

Rostrocaudal dispersion is observed in clones derived from an earlier precursor, because rare and very large clones at E8.5 colonise the entire length of the cardiac tube. This suggests that dispersive growth is continuous, and is initiated early, such that clones derived from an earlier precursor are widely distributed. A high level of intermingling has been reported to occur between mouse epiblast cells, shortly before and during gastrulation (Lawson et al., 1991; Gardner and Cockroft, 1998), suggesting that dispersion between myocardial precursor cells may be initiated in the epiblast, between E6 and E7. Cardiac precursor cells ingress through the primitive streak at E7 (Kinder et al., 1999). Later, as these cells migrate rostrally, they may also intermingle. Although this is controversial, it has been observed in chick (DeHaan, 1963a; Redkar et al., 2001) and is compatible with studies of chick gastrulation movements (Yang et al., 2002). Rostrocaudal dispersion was indeed observed in four hearts at E8.5 containing six to eight labelled cells, indicating that dispersive growth is still operational three divisions earlier than E8.5, and suggesting that it continues after gastrulation. Therefore, the idea that myocardial precursor cells grow and move as a coherent sheet from the primitive streak to the heart tube (Rosenquist and De Haan, 1966; Stalsberg and De Haan, 1969) is not compatible with our results.

A similar process of early rostrocaudal dispersion has been reported in several other epithelial structures in the mouse embryo, including endoderm (Lawson and Pedersen, 1987), notochord (Lawson and Pedersen, 1992; Beddington, 1994), myotome (Nicolas et al., 1996; Eloy-Trinquet and Nicolas, 2002) and neuroepithelium (Lawson and Pedersen, 1992; Mathis and Nicolas, 2000; Mathis et al., 1999). It is therefore possible that the early rostrocaudal dispersive phase of myocardial precursor cell growth is regulated by a general organising signal, such as that emanating from the node or the primitive streak, leading to the rostrocaudal elongation of structures in the developing embryo.

Growth transition at the time of heart tube formation

The coherent growth phase of myocardial cells has already been initiated at E8.5 as 64% of the hearts at this stage contain coherent clones (single cluster). Our analysis at E8.5 shows that there is heterogeneity in the growth properties of the precursors of the clusters. This may be due to differential growth rates. However, previous reports in chick embryos, based on tritiated thymidine incorporation, did not detect differences in the rate of proliferation of cardiac cells in the early cardiac tube (Sissman, 1966). The heterogeneity may

instead be due to an asynchronous transition from dispersive to coherent growth. Indeed, during the early phases of cardiogenesis, new cardiac precursor cells are being continuously added to the myocardium, rostrally and caudally to both poles of the heart (Viragh and Challice, 1973; Kelly and Buckingham, 2002). Heterogeneity in the sizes of clusters from hearts with multiple clusters at E8.5 is observed in the different cardiac subregions (data not shown). However, the maximum size of these clusters is significantly higher in the primitive ventricle (27) than at the arterial (15) or venous (13) poles, suggesting that the first cells that undergo the transition to coherent growth are ventricular precursor cells. This is in agreement with previous in vivo labelling studies in the chick embryo, which have shown that the cardiac tube is initially mostly composed of ventricular precursor cells (de la Cruz et al., 1989). Thus, the progressive increase in differentiated myocardial cells, which occurs during the same time period, is likely to be linked with the growth phase transition.

One can only speculate at present about the molecular signals that induce this major transition in cell behaviour, which is characterised by reduced intermingling and a change in growth orientation. In addition to extrinsic signals, major cardiac transcription factors such as Nkx2.5 (Lyons et al., 1995; Tanaka et al., 1999) may be implicated in this process. It is only after formation of the cardiac tube that null mutations in this gene and in those encoding factors such as Hand1 or Hand2 (Srivastava et al., 1997; Firulli et al., 1998; Riley et al., 1998), or Tbx5 (Bruneau et al., 2001), which are only expressed in a subset of cardiac cells, interfere with the formation of a specific cardiac chamber. These factors may affect myocardial cell growth. Indeed, Tbx5 (Hatcher et al., 2001), Hand2 (Yamagishi et al., 2001) and HOP, a recently discovered downstream effector of Nkx2.5 (Shin et al., 2002; Chen et al., 2002) have been shown to be directly involved in cell proliferation and survival.

Coherent growth of myocardial cells at the time of chamber formation

Our results show that coherent growth predominates after E8.5, at the time of chamber formation. Indeed, between E8.5 and E10.5, the number of cells per cluster in hearts with multiple clusters increases. This is consistent with previous observations of chick ventricular cell growth, based on retroviral labelling at different developmental stages (Mikawa et al., 1992a). However, coherent growth is not confined to the cardiac chambers and is therefore not a specific characteristic of the proliferative (‘working’) myocardium which has been proposed to balloon out from the outer curvature of the primitive cardiac tube (Christoffels et al., 2000). Nor is it confined to myocardial cells derived from the primary, as distinct from the anterior or secondary heart field, which provides myocardial precursors for the outflow tract region of the heart during this period (Kelly et al., 2001). Coherent growth is observed at E10.5 and at later stages in all regions of the heart.

We show that myocardial cells follow a proliferative mode of growth with an apparent growth rate of 15 hours per cell cycle between E8.5 and E10.5. This growth rate is not significantly different from that proposed in chick (Mikawa et al., 1992a; Mima et al., 1995) and is higher than that calculated previously in the mouse heart at E9 and E10, based on tritiated thymidine incorporation (10 hours) (see Rumyantsev, 1977). This is only an approximation, as BrdU labelling showed similar levels of proliferation in the primitive chambers but lower levels in the inner curvature of the tubular heart as it loops. The atrioventricular canal and distal truncus have fewer dividing cells, but it is only later, as septation takes place, that major changes occur in the chick (Thompson et al., 1990) and mouse (see Rumyantsev, 1977) hearts. Selective cell death, during remodelling of the outflow tract for example, is again a later phenomenon. At early stages of cardiogenesis apoptosis is confined to small areas, along the midline of the fusing heart tube and at the poles when the tube detaches from the body (van den Hoff et al., 2000; Cheng et al., 2002). We find that clone size and numbers increase between E8.5 and E10.5 throughout the heart and we therefore do not detect a major impact of cell cycle withdrawal or apoptosis during this period. Together, these observations indicate that differential rates of proliferation and selective cell death may modulate growth parameters locally in rare clones but are unlikely to introduce a major bias in the overall growth characteristics that we describe here at embryonic stages.

As in the case of the chick heart (Mikawa et al., 1992a), we observe wedge-shaped clusters across the ventricular wall. This would imply that cells have proliferated more in the peripheral layer of the myocardium, which is supported by the distribution of BrdU negative quiescent cells (Thompson et al., 1990) (see Mikawa et al., 1992a), and would be important in shaping the ventricular chambers. In considering how the ventricles grow, it is notable that clones of labelled cells extend from compact to trabeculated myocardium and also from the trabeculae to the muscular part of the interventricular septum, implying that this is a clonal continuum.

In most clusters, as early as E10.5, coherent growth is characterised by an elongated geometry and a suborganisation into rows of cells, both on the surface of the heart and traversing the ventricular wall. There is some degree of intermingling with occasional non-labelled cells within the β-galactosidase-positive clone. These observations are in accordance with those of Mikawa et al. (Mikawa et al., 1992a) who described similar growth characteristics across the adult chick ventricular wall. They found that secondary rows of cells or ‘minispindles’ were orientated at 20-40° to the main axis of elongation, or ‘masterspindle’, of the cluster. By contrast, in the mouse heart, where we document this phenomenon throughout the myocardium, the axis of the rows of cells appears to be random in relation to the main axis of the cluster. This would suggest that two independent events of orientation are occurring simultaneously during the growth of a cluster. Indeed, no large single row of cells was observed. The local signals responsible for the orientation of the rows and for the elongation of the clusters remain to be determined but this organisation of cell growth within a cluster is no doubt an important, characteristic aspect of cardiac morphogenesis. In clusters at P7, the orientation of the rows of cells appears to correlate with that of cardiac myofibres. This is compatible with our observation of a progressive shift in their orientation across the ventricular wall and consistent with the description of ‘minispindles’ in chick (Mikawa et al., 1992a). Our results in the mouse imply that a myofibre is polyclonal and that architecture is prefigured in the embryonic heart as early as E10.5, by the orientation of cell division, reflected by the arrays

of nuclei seen in a cluster. This is in contrast to the later appearance of a supracellular organisation of the sarcomeres at E15 described for the rat embryo (Wenink et al., 1996). A possible signal for the orientation of the rows of cells may originate from mechanical forces, created by tissue contraction and blood pressure, that are thought to influence myocardial architecture (see Taber, 1998; Sedmera et al., 2000). Such signals would be independent from molecular signals regulating cardiomyocyte proliferation. Relevant to this, missense mutations in sarcomeric genes such as α-cardiac actin, have been shown to lead to hypertrophic cardiomyopathies characterised by myocardial fibre disarray and cell disorganisation (Bonne et al., 1998).

Conclusions

Clonal analysis of myocardial cells in the mouse heart has revealed two growth phases with an asyonchronous transition between different myocardial cell precursors, during the period of cardiac tube formation and of progressive cardiac cell differentiation. The first dispersive phase marks the early stages of cardiogenesis. The second coherent phase of cell growth characterises all regions of the myocardium and coincides with the major remodelling of the cardiac tube and subsequent growth of the four-chambered heart. Notably, the myofibre architecture of the mouse heart would appear to be prefigured at E10.5, by oriented cell proliferation, and this has potential implications for cardiomyopathies. Comparison with observations on the chick heart would suggest that characteristics of coherent growth are well conserved in amniotes. It will be of major interest to assess the extent of conservation of the dispersive growth phase in the chick and other vertebrates. One can speculate about its importance in hearts, like that of the zebrafish, which remains as a tube with a single ventricle and atrium, and in which mutations in genes such as *tbx5* (Garrity et al., 2002) or *hand2* (Yelon et al., 2000) have a much more severe phenotype. Indeed single cell injection into the early blastula of zebrafish resulted in clones of 2-22 cells distributed rostrocaudally along the extent of the heart tube at 36 hpf (Stainier et al., 1993). These observations point to the interest of pursuing the characterisation of cell growth modes in order to understand the mechanisms underlying heart morphogenesis and evolution.

We are grateful to L. Mathis for many helpful discussions, to A. Munk and N. Brown for comments on the manuscript, and to M. van den Hoff for providing missing references. We thank C. Bodin and E. Pecnard for technical assistance. We also thank our colleagues for the gift of plasmids, J. Lessard for sharing sequence data and Y. Lallemand for providing the PGK-Cre transgenic mouse strain. Our work is supported by the Pasteur Institute, the Centre National de la Recherche Scientifique and the ACI programme in Integrative Biology of the French Ministry of Research (MJER). S.M. has benefitted from a fellowship from the MJER and the University of Paris (monitorat). R.K. is an INSERM research fellow. S.E.-T. is grateful to the ARC and AFM for support.

REFERENCES

Beddington, R. S. (1994). Induction of a second neural axis by the mouse node. *Development* **120**, 613-620.

Biben, C., Hadchouel, J., Tajbakhsh, S. and Buckingham, M. (1996). Developmental and tissue-specific regulation of the murine cardiac actin gene in vivo depends on distinct skeletal and cardiac muscle-specific enhancer elements in addition to the proximal promoter. *Dev. Biol.* **173**, 200-212.

Bonne, G., Carrier, L., Richard, P., Hainque, B. and Schwartz, K. (1998). Familial hypertrophic cardiomyopathy: from mutations to functional defects. *Circ. Res.* **83**, 580-593.

Bonnerot, C. and Nicolas, J. F. (1993). Clonal analysis in the intact mouse embryo by intragenic homologous recombination. *C. R. Acad. Sci. III* **316**, 1207-1217.

Bruneau, B. G., Nemer, G., Schmitt, J. P., Charron, F., Robitaille, L., Caron, S., Conner, D. A., Gessler, M., Nemer, M., Seidman, C. E. et al. (2001). A murine model of Holt-Oram syndrome defines roles of the T-box transcription factor Tbx5 in cardiogenesis and disease. *Cell* **106**, 709-721.

Burns, J. L. and Hassan, A. B. (2001). Cell survival and proliferation are modified by insulin-like growth factor 2 between days 9 and 10 of mouse gestation. *Development* **128**, 3819-3830.

Capdevila, J., Vogan, K. J., Tabin, C. J. and Izpisua Belmonte, J. C. (2000). Mechanisms of left-right determination in vertebrates. *Cell* **101**, 9-21.

Chen, F., Kook, H., Milewski, R., Gitler, A., Lu, M., Li, J., Nazarian, R., Schnepp, R., Jen, K., Biben, C. et al. (2002). Hop is an unusual homeobox gene that modulates cardiac development. *Cell* **110**, 713.

Cheng, G., Wessels, A., Gourdie, R. G. and Thompson, R. P. (2002). Spatiotemporal and tissue specific distribution of apoptosis in the developing chick heart. *Dev. Dyn.* **223**, 119-133.

Christoffels, V. M., Habets, P. E., Franco, D., Campione, M., de Jong, F., Lamers, W. H., Bao, Z. Z., Palmer, S., Biben, C., Harvey, R. P. et al. (2000). Chamber formation and morphogenesis in the developing mammalian heart. *Dev. Biol.* **223**, 266-278.

Cripps, R. M. and Olson, E. N. (2002). Control of cardiac development by an evolutionarily conserved transcriptional network. *Dev. Biol.* **246**, 14-28.

de la Cruz, M., Sanchez-Gomez, C. and Palomino, M. (1989). The primitive cardiac regions in the straight heart tube (stage 9–) and their anatomical expression in the mature heart: an experimental study in the chick embryo. *J. Anat.* **165**, 121-131.

DeHaan, R. L. (1963a). Migration patterns of the precardiac mesoderm in the early chick embryo. *Exp. Cell Res.* **29**, 544-560.

DeHaan, R. L. (1963b). Organization of the cardiogenic plate in the early chick embryo. *Acta Embryol. Morphol. Exp.* **6**, 26-38.

Eloy-Trinquet, S. and Nicolas, J. F. (2002). Cell coherence during production of the presomitic mesoderm and somitogenesis in the mouse embryo. *Development* **129**, 3609-3619.

Firulli, A. B., McFadden, D. G., Lin, Q., Srivastava, D. and Olson, E. N. (1998). Heart and extra-embryonic mesodermal defects in mouse embryos lacking the bHLH transcription factor Hand1. *Nat. Genet.* **18**, 266-270.

Fishman, M. and Olson, E. (1997). Parsing the heart: genetic modules for organ assembly. *Cell* **91**, 153-156.

Garcia-Martinez, V. and Schoenwolf, G. C. (1993). Primitive-streak origin of the cardiovascular system in avian embryos. *Dev. Biol.* **159**, 706-719.

Gardner, R. L. and Cockroft, D. L. (1998). Complete dissipation of coherent clonal growth occurs before gastrulation in mouse epiblast. *Development* **125**, 2397-2402.

Garrity, D. M., Childs, S. and Fishman, M. C. (2002). The heartstrings mutation in zebrafish causes heart/fin Tbx5 deficiency syndrome. *Development* **129**, 4635-4645.

Harvey, R. P. (2002). Organogenesis: Patterning the vertebrate heart. *Nat. Rev. Genet.* **3**, 544-556.

Hatcher, C. J., Kim, M. S., Mah, C. S., Goldstein, M. M., Wong, B., Mikawa, T. and Basson, C. T. (2001). TBX5 transcription factor regulates cell proliferation during cardiogenesis. *Dev. Biol.* **230**, 177-188.

Kelly, R. G., Brown, N. A. and Buckingham, M. E. (2001). The arterial pole of the mouse heart forms from Fgf10-expressing cells in pharyngeal mesoderm. *Dev. Cell* **1**, 435-440.

Kelly, R. G. and Buckingham, M. E. (2002). The anterior heart-forming field: voyage to the arterial pole of the heart. *Trends Genet.* **18**, 210-216.

Kinder, S. J., Tsang, T. E., Quinlan, G. A., Hadjantonakis, A. K., Nagy, A. and Tam, P. P. (1999). The orderly allocation of mesodermal cells to the extraembryonic structures and the anteroposterior axis during gastrulation of the mouse embryo. *Development* **126**, 4691-4701.

Kumar, A., Crawford, K., Close, L., Madison, M., Lorenz, J., Doetschman, T., Pawlowski, S., Duffy, J., Neumann, J., Robbins, J. et al. (1997). Rescue of cardiac alpha-actin-deficient mice by enteric smooth muscle gamma-actin. *Proc. Natl. Acad. Sci. USA* **94**, 4406-4411.

Lallemand, Y., Luria, V., Haffner-Krausz, R. and Lonai, P. (1998).

Maternally expressed PGK-Cre transgene as a tool for early and uniform activation of the Cre site-specific recombinase. *Transgenic Res.* **7**, 105-112.

Lawson, K. A. and Pedersen, R. A. (1987). Cell fate, morphogenetic movement and population kinetics of embryonic endoderm at the time of germ layer formation in the mouse. *Development* **101**, 627-652.

Lawson, K. A. and Pedersen, R. A. (1992). Clonal analysis of cell fate during gastrulation and early neurulation in the mouse. *Ciba Found. Symp.* **165**, 3-26.

Lawson, K. A., Meneses, J. J. and Pedersen, R. A. (1991). Clonal analysis of epiblast fate during germ layer formation in the mouse embryo. *Development* **113**, 891-911.

Luria, S. and Delbrück, M. (1943). Mutations of bacteria from virus sensitivity to virus resistance. *Genetics* **28**, 491-511.

Lyons, I., Parsons, L. M., Hartley, L., Li, R., Andrews, J. E., Robb, L. and Harvey, R. P. (1995). Myogenic and morphogenetic defects in the heart tubes of murine embryos lacking the homeo box gene Nkx2-5. *Genes Dev.* **9**, 1654-1666.

Mathis, L. and Nicolas, J. F. (2000). Different clonal dispersion in the rostral and caudal mouse central nervous system. *Development* **127**, 1277-1290.

Mathis, L. and Nicolas, J. F. (2002). Cellular patterning of the vertebrate embryo. *Trends Genet.* **18**, 627-635.

Mathis, L., Sieur, J., Voiculescu, O., Charnay, P. and Nicolas, J. F. (1999). Successive patterns of clonal cell dispersion in relation to neuromeric subdivision in the mouse neuroepithelium. *Development* **126**, 4095-4106.

Mikawa, T., Borisov, A., Brown, A. M. and Fischman, D. A. (1992a). Clonal analysis of cardiac morphogenesis in the chicken embryo using a replication-defective retrovirus: I. Formation of the ventricular myocardium. *Dev. Dyn.* **193**, 11-23.

Mikawa, T., Cohen-Gould, L. and Fischman, D. A. (1992b). Clonal analysis of cardiac morphogenesis in the chicken embryo using a replication-defective retrovirus. III: Polyclonal origin of adjacent ventricular myocytes. *Dev. Dyn.* **195**, 133-141.

Mima, T., Ueno, H., Fischman, D. A., Williams, L. T. and Mikawa, T. (1995). Fibroblast growth factor receptor is required for in vivo cardiac myocyte proliferation at early embryonic stages of heart development. *Proc. Natl. Acad. Sci. USA* **92**, 467-471.

Mjaatvedt, C. H., Nakaoka, T., Moreno-Rodriguez, R., Norris, R. A., Kern, M. J., Eisenberg, C. A., Turner, D. and Markwald, R. R. (2001). The outflow tract of the heart is recruited from a novel heart-forming field. *Dev. Biol.* **238**, 97-109.

Nicolas, J. F., Mathis, L., Bonnerot, C. and Saurin, W. (1996). Evidence in the mouse for self-renewing stem cells in the formation of a segmented longitudinal structure, the myotome. *Development* **122**, 2933-2946.

Olson, E., Arnold, H., Rigby, P. and Wold, B. (1996). Know your neighbors: three phenotypes in null mutants of the myogenic bHLH gene MRF4. *Cell* **85**, 1-4.

Rawles, M. E. (1943). The heart-forming areas of the early chick blastoderm. *Physiol. Zool.* **16**, 22-42.

Redkar, A., Montgomery, M. and Litvin, J. (2001). Fate map of early avian cardiac progenitor cells. *Development* **128**, 2269-2279.

Riley, P., Anson-Cartwright, L. and Cross, J. C. (1998). The Hand1 bHLH transcription factor is essential for placentation and cardiac morphogenesis. *Nat. Genet.* **18**, 271-275.

Rosenquist, G. C. and De Haan, R. L. (1966). Migration of precardiac cells in the chick embryo: a radioautographic study. *Contribut. Embryol.* **263**, 111-121.

Rumyantsev, P. P. (1977). Interrelations of the proliferation and differentiation processes during cardiact myogenesis and regeneration. *Int. Rev. Cytol.* **51**, 186-273.

Sassoon, D. A., Garner, I. and Buckingham, M. (1988). Transcripts of alpha-cardiac and alpha-skeletal actins are early markers for myogenesis in the mouse embryo. *Development* **104**, 155-164.

Sedmera, D., Pexieder, T., Vuillemin, M., Thompson, R. P. and Anderson, R. H. (2000). Developmental patterning of the myocardium. *Anat. Rec.* **258**, 319-337.

Selfridge, J., Pow, A. M., McWhir, J., Magin, T. M. and Melton, D. W. (1992). Gene targeting using a mouse HPRT minigene/HPRT-deficient embryonic stem cell system: inactivation of the mouse ERCC-1 gene. *Somat. Cell Mol. Genet.* **18**, 325-336.

Shin, C., Liu, Z., Passier, R., Zhang, C., Wang, D., Harris, T., Yamagishi, H., Richardson, J., Childs, G. and Olson, E. (2002). Modulation of cardiac growth and development by HOP, an unusual homeodomain protein. *Cell* **110**, 725.

Sissman, N. J. (1966). Cell multiplication rates during development of the primitive cardiac tube in the chick embryo. *Nature* **210**, 504-507.

Soriano, P. (1997). The PDGF alpha receptor is required for neural crest cell development and for normal patterning of the somites. *Development* **124**, 2691-2700.

Srivastava, D., Thomas, T., Lin, Q., Kirby, M. L., Brown, D. and Olson, E. N. (1997). Regulation of cardiac mesodermal and neural crest development by the bHLH transcription factor dHAND. *Nat. Genet.* **16**, 154-160.

Stainier, D. Y., Lee, R. K. and Fishman, M. C. (1993). Cardiovascular development in the zebrafish. I. Myocardial fate map and heart tube formation. *Development* **119**, 31-40.

Stalsberg, H. and De Haan, R. L. (1969). The precardiac areas and formation of the tubular heart in the chick embryo. *Dev. Biol.* **19**, 128-159.

Stent, G. S. (1985). The role of cell lineage in development. *Philos. Trans. R. Soc. Lond. B. Biol. Sci.* **312**, 3-19.

Taber, L. A. (1998). Mechanical aspects of cardiac development. *Prog. Biophys. Mol. Biol.* **69**, 237-255.

Tajbakhsh, S., Bober, E., Babinet, C., Pournin, S., Arnold, H. and Buckingham, M. (1996a). Gene targeting the myf-5 locus with nlacZ reveals expression of this myogenic factor in mature skeletal muscle fibres as well as early embryonic muscle. *Dev. Dyn.* **206**, 291-300.

Tajbakhsh, S., Rocancourt, D. and Buckingham, M. (1996b). Muscle progenitor cells failing to respond to positional cues adopt non-myogenic fates in myf-5 null mice. *Nature* **384**, 266-270.

Tam, P. P., Parameswaran, M., Kinder, S. J. and Weinberger, R. P. (1997). The allocation of epiblast cells to the embryonic heart and other mesodermal lineages: the role of ingression and tissue movement during gastrulation. *Development* **124**, 1631-1642.

Tanaka, M., Chen, Z., Bartunkova, S., Yamasaki, N. and Izumo, S. (1999). The cardiac homeobox gene Csx/Nkx2.5 lies genetically upstream of multiple genes essential for heart development. *Development* **126**, 1269-1280.

Thomas, K. R., Folger, K. R. and Capecchi, M. R. (1986). High frequency targeting of genes to specific sites in the mammalian genome. *Cell* **44**, 419-428.

Thompson, R. P., Lindroth, J. R. and Wong, Y. M. M. (1990). Regional differences in DNA-synthetic activity in the preseptation myocardium of the chick. In *Developmental Cardiology: Morphogenesis and Function* (ed. E. B. Clark and A. Takao), pp. 219-234. Mount Kisco, NY: Futura Publishing.

van den Hoff, M. J., van den Eijnde, S. M., Viragh, S. and Moorman, A. F. (2000). Programmed cell death in the developing heart. *Cardiovasc. Res.* **45**, 603-620.

Viragh, S. and Challice, C. E. (1973). Origin and differentiation of cardiac muscle cells in the mouse. *J. Ultrastruct. Res.* **42**, 1-24.

Waldo, K. L., Kumiski, D. H., Wallis, K. T., Stadt, H. A., Hutson, M. R., Platt, D. H. and Kirby, M. L. (2001). Conotruncal myocardium arises from a secondary heart field. *Development* **128**, 3179-3188.

Wenink, A. C., Knaapen, M. W., Vrolijk, B. C. and VanGroningen, J. P. (1996). Development of myocardial fiber organization in the rat heart. *Anat. Embryol.* **193**, 559-567.

Yamagishi, H., Yamagishi, C., Nakagawa, O., Harvey, R. P., Olson, E. N. and Srivastava, D. (2001). The combinatorial activities of Nkx2.5 and dHAND are essential for cardiac ventricle formation. *Dev. Biol.* **239**, 190-203.

Yang, X., Dormann, D., Munsterberg, A. E. and Weijer, C. J. (2002). Cell movement patterns during gastrulation in the chick are controlled by positive and negative chemotaxis mediated by FGF4 and FGF8. *Dev. Cell* **3**, 425-437.

Yelon, D., Ticho, B., Halpern, M. E., Ruvinsky, I., Ho, R. K., Silver, L. M. and Stainier, D. Y. (2000). The bHLH transcription factor hand2 plays parallel roles in zebrafish heart and pectoral fin development. *Development* **127**, 2573-2582.

Zaffran, S. and Frasch, M. (2002). Early signals in cardiac development. *Circ. Res.* **91**, 457-469.

Zammit, P. S., Kelly, R. G., Franco, D., Brown, N., Moorman, A. F. and Buckingham, M. E. (2000). Suppression of atrial myosin gene expression occurs independently in the left and right ventricles of the developing mouse heart. *Dev. Dyn.* **217**, 75-85.